Molecular Crystals and Liquid Crystals

Publication details, including instructions for authors and subscription information:
http://www.tandfonline.com/loi/gmcl20

π-Conjugated Triphenylene Twins Exhibiting Polymesomorphism Including the Nematic Phase

Sanjay Kumar Varshney [a], Hideo Takezoe [b], Veena Prasad [a] & D. S. Shankar Rao [a]

[a] Centre for Liquid Crystal Research, Jalahalli, Bangalore, India

[b] Department of Organic and Polymeric Materials, Tokyo Institute of Technology, O-okayama, Meguro-ku, Tokyo, Japan

Version of record first published: 17 Dec 2009

To cite this article: Sanjay Kumar Varshney, Hideo Takezoe, Veena Prasad & D. S. Shankar Rao (2009): π-Conjugated Triphenylene Twins Exhibiting Polymesomorphism Including the Nematic Phase, Molecular Crystals and Liquid Crystals, 515:1, 16-38

To link to this article: http://dx.doi.org/10.1080/15421400902987677

Mol. Cryst. Liq. Cryst., Vol. 515, pp. 16–38, 2009

ISSN: 1542-1406 print/1563-5287 online
DOI: 10.1080/15421400902987677

Taylor & Francis
Taylor & Francis Group

π-Conjugated Triphenylene Twins Exhibiting Polymesomorphism Including the Nematic Phase

Sanjay Kumar Varshney[1], Hideo Takezoe[2], Veena Prasad[1], and D. S. Shankar Rao[1]
[1]Centre for Liquid Crystal Research, Jalahalli, Bangalore, India
[2]Department of Organic and Polymeric Materials, Tokyo Institute of Technology, O-okayama, Meguro-ku, Tokyo, Japan

Novel discotic liquid crystals possessing two triphenylene (TP) mesogenic cores covalently connected via a rigid spacer, i.e., π-conjugated ethynyl- or butadiynyl-bridge, (TP twins) are reported. The TP twins are categorized by the lengths of β-substituted chains (R_2 and R_3) and peripheral alkoxy or branched aliphatic chains (R_1 and R_4). Three varieties of TP twins are prepared: A) TP twins having identical β-substituted and peripheral chains ($R_1 = R_2 = R_3 = R_4$), B) equivalent TP entities having a β-substituted chain ($R_2 = R_3$) and peripheral chains ($R_1 = R_4$) of different length from the β substitution, and C) TP twins with different TP entities having the same β-substituted and peripheral alkoxy chains ($R_1 = R_2$, $R_3 = R_4$). The phase behavior is characterized by differential scanning calorimetry (DSC), polarizing optical microscopy (POM) and X-ray diffraction (XRD) studies. These TP twins exhibit a discotic nematic (N) and/or columnar rectangular (Col_r) mesophases over a wide temperature range. We found that the relative length of rigid spacer and β-substituted alkoxy chains play an important role in the creation of the molecular self-assembly and formation of the mesophases. To the best of our knowledge, this is the first report of TP twins exhibiting polymesomorphism.

Keywords: discotic nematic phase; polymesomorphism; triphenylene; twin dimer

1. INTRODUCTION

The π-conjugated organic materials strongly support the better-performing electronic devices for the rapidly-growing technology [1]. The performance of electronic devices using organic materials depends on their chemical structures, purity of materials, supramolecular

Address correspondence to Hideo Takezoe, Department of Organic and Polymeric Materials, Tokyo Institute of Technology, O-okayama 2-12-1, Meguro-ku, Tokyo 152-8552, Japan. E-mail: takezoe.h.aa@m.titech.ac.jp

assemblies, etc. The organic materials have several advantages over inorganic materials that lead to the constant demand of better-performing electronic devices [2]. The development of discotic liquid crystals (DLCs) has been extensively made as a special category of organic optoelectronically-active, "soft-materials" [3], and DLCs are now recognized as important materials for applications in the rapidly-growing nano-science, technology and electronic industry [3]. The physical characteristics of DLCs in columnar hierarchy are very promising for higher charge carrier mobility [4–7]. The columnar mesophase provides several advantages such as their relatively easy synthesis, easy processability, self-organization within their mesophases, high anisotropy of specific properties [8], etc. Other most prominent characteristics are organic field effect transistors (OFETs), photovoltaic solar cells, organic light emitting diodes (OLEDs) [9–15], etc. In addition, since DLCs have the negative anisotropy of refractive index, discotic nematic LCs are used to compensate the positive anisotropy of LCs and to improve the viewing angle characteristics of LC displays [16–19]. The most promising DLCs widely range in compounds with aromatic and polyaromatic cores such as benzene, hexa-*peri*-hexabenzocoronene, dibenzopyrene, phthalocyanine, perylene, triphenylene (TP), etc. [20,21].

Disc-shaped molecules primarily form two types of mesophases: columnar (Col) and nematic (N). It is often easy to design the DLCs exhibiting Col phase with basic structural features, flat or nearly flat aromatic core surrounded by several flexible side tails, whereas it is rather difficult to design molecules which can form the N phase. On the other hand, discotic dimers, twins, or oligomers display unique mesomorphism and are model compounds for LC-polymers. Comparing the large number of LC twins consisting of two rod-like mesogens, the number of discotic twins is very small. Among these polyaromatic cores, only TP is widely investigated and its chemical features have been often reviewed [20,22]. Although a large number of TP derivatives form the Col phase, only a small number of members exhibit the N phase [22–24]. Symmetrical or non-symmetrical TP twins, in which two TP moieties are connected via a variety of flexible spacer, have been reported, but they exhibit only Col_h and glassy state [25–31]. The chemical and thermal properties of the TP twins, oligomers, and polymers have been reviewed recently. To the best of our knowledge there is no report that the TP twins or oligomers show polymesomorphism, such as Col_r and N.

The spacer length plays a significant role in the mesophase formation of the twin. Only the twins, in which the length of the flexible spacer fulfills the space filling model, show the mesomorphism.

Variations in molecular geometry are required to alter the mesophase significantly, and only slight variations in disc-shaped molecules sometimes bring about polymesomorphism. Two TP moieties are not coplanar due to the steric crowdedness. If the molecules have sufficient flexibility, two TP moieties can be stacked on each other or in adjacent columns (Fig. 1). We propose that linking two TP molecules via a rigid spacer may experience some steric hindrance to avoid overlapping of aliphatic peripheral chains and a weak distortion of the planarity of the core. This may reduce intracolumnar interactions. The rigid molecules assemble themselves [32] into two-dimensional (2D) lattice, so that they may form the columnar phase, or stay in more or less parallel position having orientational order with smaller long-range positional order, likely forming, therefore, the N mesophase [33,34]. In some cases, molecules may show both or more phases; i.e., polymesomorphism. Even more, depending on the existence of the directional order of the rigid linkage, not only the uniaxial but also biaxial N phases may emerge (Fig. 1). Kumar and Varshney [33] synthesized TP twins rigidly linked by a butadiynyl-bridge, showing

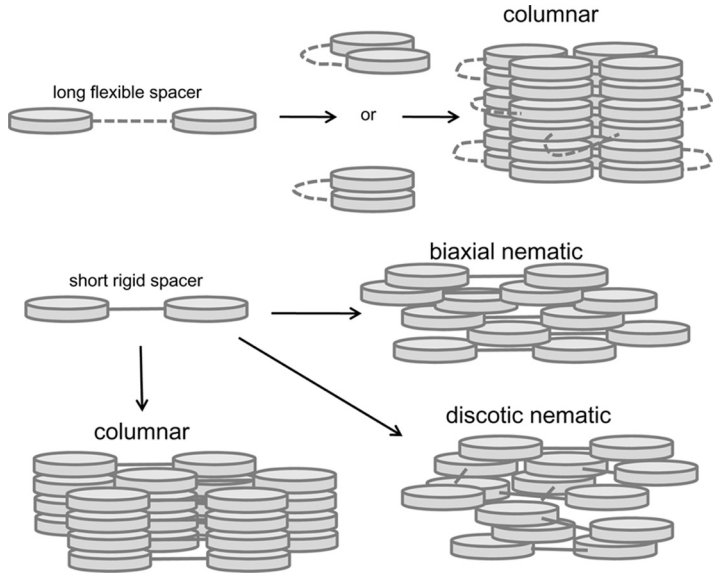

FIGURE 1 Possible structures of molecular self-assembly of triphenylene (TP) twins. Only the columnar phases, which may have inter- and intracolumnar linkages, have been found in TP twins with flexible spacers. For TP twins with rigid spacers, biaxial N phase is possible in addition to a simple uniaxial discotic N phase and columnar phase.

only the N mesophase. To examine and extend this idea, we connected two well-known liquid crystalline TP molecules showing the Col_h mesophase via π-conjugated rigid spacer, as ethynyl- or butadiynyl-bridge. The length of this rigid spacer can increase in multifold by classical chemistry [35]. Here we report the preparation and characterization of these two chemically different TP twins.

2. RESULTS AND DISCUSSION

Synthesis

To study the mesomorphic properties of the TP twins, two chemically different twins were prepared. In the first type, two TP entities are linked with ethynyl-bridge (compounds **3**) and second type having butadiynyl-bridge linkage (compounds **4**), as shown in Scheme 1. Peripheral alkoxy substitutions are grouped into three depending on the lengths of β-substituted chain of one TP (R_2) and that of another TP (R_3) and peripheral alkoxy chains of one TP (R_1) and those of another TP (R_4) (see Scheme 1): A) TP twins having identical β-substituted and peripheral alkoxy chains ($R_1 = R_2 = R_3 = R_4$; **a**∼**f**), B) Equivalent TP entities having a β-substituted alkoxy chain ($R_2 = R_3$) and peripheral alkoxy chains ($R_1 = R_4$) of different length from the β-substitution (**g**∼**k**), C) TP twins with different TP entities having the same β-substituted and peripheral alkoxy chains ($R_1 = R_2$, $R_3 = R_4$; **l**). Note that most of the substituted chains (**a**∼**f**, **h**∼**j**, **k**, **l**) are normal and/or branched alkoxy ($-OC_nH_{2n+1}$) except for **g** (−H). As for branched chains, the longest length of the branched chains has eight C's for **f** and **i**, and six C's for **j**.

The preparation of DLC materials (especially twins) based on TP is often very simple but the purification are very difficult, tedious and consume a lot of time, so that the overall yield often decreases drastically. The key intermediate β-iodopentakis(alkoxy)TP (**TP-I**) and β-bromopentakis(alkoxy)TP (**TP-Br**) were synthesized by oxidative coupling of tetraalkoxybiphenyl with β-bromoalkoxybenzene as reported [36–39]. The synthesis of β-ethynylpentakis(alkoxy)TP (**2**) is outlined in the scheme. The Sonogashira coupling of **TP-Br** or **TP-I** with 2-methyl-3-butyne-2-ol yielded protective acetylene (**1**) followed by hydrolysis. It yielded the key intermediate **2**. The target twins having ethynyl-bridge (**3**) were synthesized by Sonogashira coupling. Twins having butadiynyl-bridge (**4**) were synthesized by Glasser-Hey metal mediated coupling [40–43]. The synthesis of these two chemically different twins is shown in the scheme. The chemical structure of all new molecules was confirmed by the spectroscopic and spectrometric analyses.

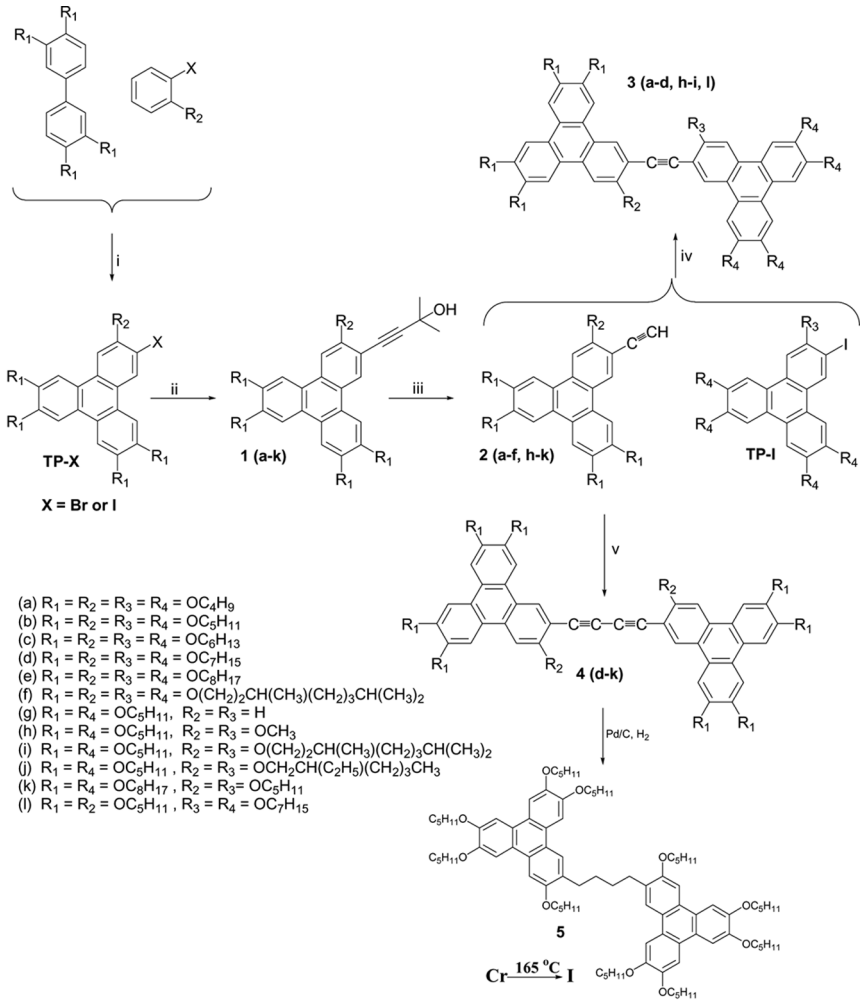

[a] Key : (i) $MoCl_5$, CH_2Cl_2, MeOH ; (ii) 2-methyl-3-butyne-2-ol, $Pd[Cl_2(PPh_3)_2]$, CuI, PPh_3, Et_3N, 80 °C, 24h; (iii) KOH, PhMe, 80 °C 2h; (iv) $Pd[Cl_2(PPh_3)_2]$, CuI, PPh_3, Et_3N, 80 °C, 36h ; (v) Cu(OAc), Py., THF, MeOH, 80 °C 24h

SCHEME 1 Synthesis of triphenylene twins[a]. The TP twins with a short linkage (**3**), a long linkage (**4**), and a flexible linkage (**5**) were used in the present experiment. As peripheral substituted chains, alkoxy or aliphatic chains (**a–l**) were used. The compounds are categorized into three; type A (**a–f**), type B (**g–k**), and type C (**l**).

Liquid Crystalline Properties

The mesogenic properties of all the TP twins were investigated by polarizing optical microscopy (POM), differential scanning calorimetry

(DSC), and X-ray diffraction (XRD) studies. The second heating and cooling data of DSC scans are summarized in Table 1, which includes data from a previous report [33]. The phases were identified by POM and XRD. Let us first describe twins having the same peripheral alkoxy tails (type A: **3a**–**3d**, **4d**, and **4f**). The POM observation of twin **3a** showed the fluid N phase with schlieren texture. The next-higher homologue **3b** showed only the N phase on heating. On cooling, the schlieren texture of the N phase changed to dendritic texture in the Col_r phase, as shown in Fig. 2(a). The N-Col_r transition was confirmed by DSC scans (ΔH 6.5 Jg^{-1}). A higher homologue **3c** showed the same phase sequence, but the thermal range (ΔT) of the N phase decreased drastically, $\Delta T \sim 3.6^{\circ}C$ on cooling, whereas the thermal range of the Col_r phase (Fig. 2(b)) increased slightly, $\Delta T \sim 61^{\circ}C$ on cooling. The derivative **3d** showed only dendritic textures in the Col_r phase over a wide thermal range. In this way, the N phase range decreases with increasing the chain length, and instead the Col_r phase becomes stabilized.

TABLE 1 Phase Transition Temperatures and Enthalpies of Triphenylene Twins. Cr, Cr_1; Crystals, N; Nematic, Col_r; Rectangular Columnar, M_x; Mesophase Yet to be Identified, I; Isotropic

Twins	Thermal transitions/°C and enthalpy changes/J/g (in parenthes) Heating scan/Cooling scan
3a	Cr 162.8 (14.8) N 234.5 (0.44) I / I 232.4 (0.36) N 148.6 (10.2) Cr
3b	Cr 163.4 (56) N 198.4 (0.39) I / I 198 (0.3) N 161 (6.5) Col_r 115 (23) Cr
3c	Cr 147.2 (44.8) Col_r 161.6 (3.9) N 163 (0.32) I / I 162.8 (0.22) N 159.2 (5.2) Col_r 98 (38.4) Cr
3d	Cr 136.5 (42.3) Col_r 156.3 (2.4) I / I 153.8 (2.4) Col_r 93.1 (37) Cr
3h	Cr 160 (18) N 182.8 (0.05) I / I 181.8 (0.7) N 147.6 (21) Cr
3i	Cr 113.5 (36.9) Col_r 143.3 (6.9) I / I 139.9 (7.5) Col_r 76 (24.5) Cr
3l	Cr1 112 (12.7) Cr 119.3 (1.4) N 163.9 (0.23) I / I 162.9 (0.13) N 92.5 (4.1) Cr 79 (15.9) Cr_1
4a*	Cr 188.6 (18.7) N 243.5 (1.1) I / I 238.8 (0.8) N 172.8 (16.0) Cr
4b*	Cr 161.0 (19.1) N 215.9 (0.6) I / I 214.4 (0.7) N 152.8 (19.2) Cr
4c*	Cr 135.3 (22.6) N 172.8 (0.9) I / I 170.7 (0.8) N 126.5 (21.8) Cr
4d	Cr 125.4 (19.8) I / I 119.8 (0.08) N 111.2 (18.0) Cr
4e	Cr 112.4 (8.2) I
4f	Liquid
4g	Cr 189.3 (21.45) I
4h	Cr 185.7 (20.4) N 202.9 (0.63) I / I 202.1 (0.9) N 167.3 (0.32) M_x 161.6 (−8.6) Cr
4i	Cr 122.8 (0.7) Col_r 135.6 (8.7) N 149.1 (0.47) I / I 148.7 (0.47) N 132.6 (8.8) Col_r 119.7 (−5.1) Cr
4j	Cr 143.4 (8.6) N 196.2 (0.39) I / I 195.4 (0.4) N 138.0 (10.4) Cr
4k	Cr 112.9 (18.1) N 136.5 (0.27) I / I 135.6 (0.15) N 80.1 (14.3) Cr

*Data from ref. [33].

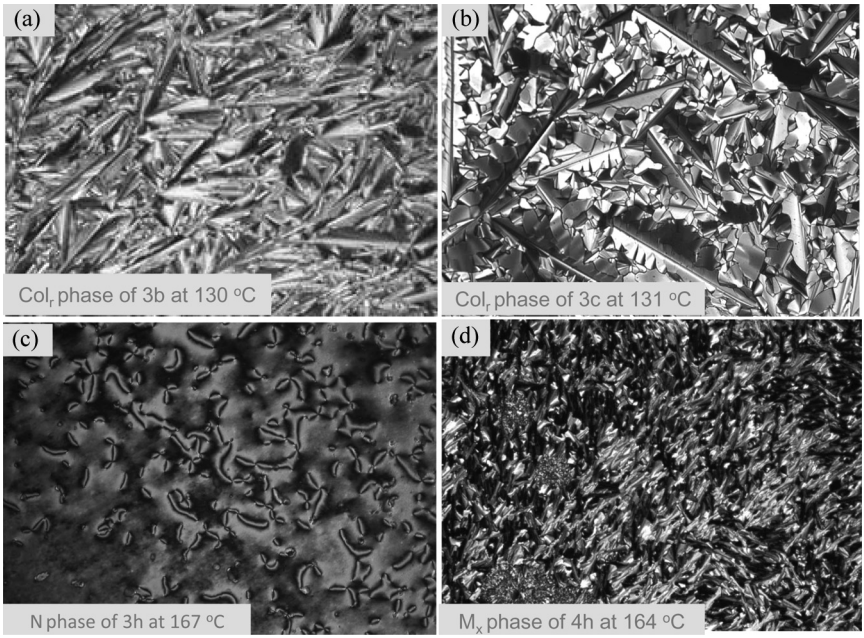

FIGURE 2 The selected optical textures of the twin **3** and twin **4** obtained on cooling from isotropic liquid, (a) Col_r phase of **3b** at 130°C, (b) Col_r phase of **3c** at 131°C, (c) N phase of **3h** at 167°C, and (d) M_x phase of **4h** at 164°C.

The situation is the same in **4a**–**4d**, except that the N phase was more stable than 3 series, and even the derivative **4d** showed the monotropic N mesophase, though the temperature range was not so wide ($\Delta T \sim 8.6$°C). Further, the homologue **4e** having longer peripheral alkoxy tails was non-mesomorphic, and **4f** having the branched aliphatic chain is liquid at room temperature (RT). Among the type A compounds with an ethynyl-bridge, it is clear that the N phase more stably exists in homologues with shorter chain lengths. For the type A compounds with a longer butadiynyl-bridge, **4d** exhibited the N phase, although **3d** with the same peripheral alkoxy tails showed no N phase. However, the N phase disappeared in longer homologue **4e** as same as the homologues **3**. Thus, the emergence of the N phase is strongly influenced by the chain length and the spacer length.

Next, in order to see which chains play a crucial rule, another type homologue, type B, were examined. Compound **3h**, which has shorter β-substituted chain together with the same other chains as **3b**, shows the N phase (Fig. 2(c)). In contrast, **3i**, which has longer β-substituted branched aliphatic chain (3,7-dimethyloctane) together with the same

other chains as **3b**, did not show the N phase, and instead exhibited the disordered Col_r mesophase. Interestingly, however, the twin **4i** having the same chain structures as **3i** exhibited the Col_r and N mesophases. The temperature ranges of the N and Col_r phases are 16.1°C and 12.9°C, respectively. The twin **4h** showed the N phase and the other phase being monotropic and having a narrow thermal range ($\Delta T \sim 5.7$°C) could not be properly characterized, and it is termed as M_x (Fig. 2(d)). The enthalpy change across the N-M_x transition was smaller ($0.3\,Jg^{-1}$) and compared with that of the I-N transition ($0.9\,Jg^{-1}$). The textural pattern remained somewhat the same throughout this mesophase range. Thus, shorter β-substituted chain length compared with the spacer length is a crucial factor to have the N phase. The twins **4i** and **4j** are not exceptional; both compounds exhibited the N phase, since the longest part of their branched chains is equivalent to $-OC_8H_{16}$ and $-OC_6H_{13}$, respectively. The N phase is more stable in **4j** having 2-ethylhexyl alkoxy group at β-position than in **4i**, having 3,7-dimethyloctane. This is partly because the effective β-substituted chain length of **4j** is shorter than **4i**. It is important to realize the difference between **4f** with the branched chains at all substituted positions and **4i** with the branched chains only at β-substituted positions in their mesomorphic properties; the former shows the liquid phase at RT, but the latter shows the N and Col_r phases. Hence the introduction of branched aliphatic chains instead of simple alkoxy chains only at β-substituted positions does not prevent molecules from showing mesogenic phases(s), whereas too many branching chains decrease the phase transition temperatures to suppress the mesogenic phases at least above RT. It is also noted that both the compounds **3l** and **4k** of type C show the N phase over wide thermal ranges ($\Delta T \sim 70.4$°C and 55.5°C, respectively), on cooling. A graphical representation of thermal range of the mesophases shown in Fig. 3 highlights the difference between these three types of chemically different twins.

XRD Study

The different mesophases were confirmed by XRD measurements. Measurements were carried out on the samples **3a, 3b, 3d, 3h, 4i**, and **4h**. Representative one-dimensional intensity vs. 2θ profiles extracted from the 2D patterns for the twins **3b** and **4i** are shown in Fig. 4. The results of these investigations are summarized in Table 2.

The XRD scans of the compound **3a** taken at 185°C and 210°C showed diffuse peaks both in small and wide angle regions. This is the characteristic of the N phase. The scan taken in the N phase of

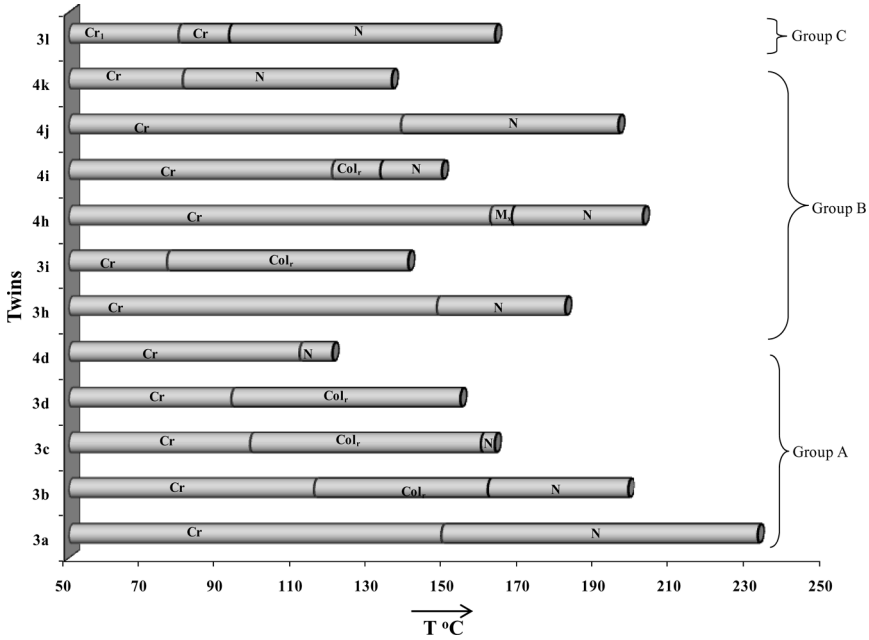

FIGURE 3 Graphical representation of the thermal ranges of mesophases of triphenylene twins of types A, B, and C.

the compound **3b** also showed the same behavior. The diffraction scan of **3b** taken at temperature 155°C showed four sharp peaks at small angles and a diffuse peak in a wide-angle region (see Fig. 4(a)). The small-angle peaks are indexed to a 2D rectangular lattice with lattice

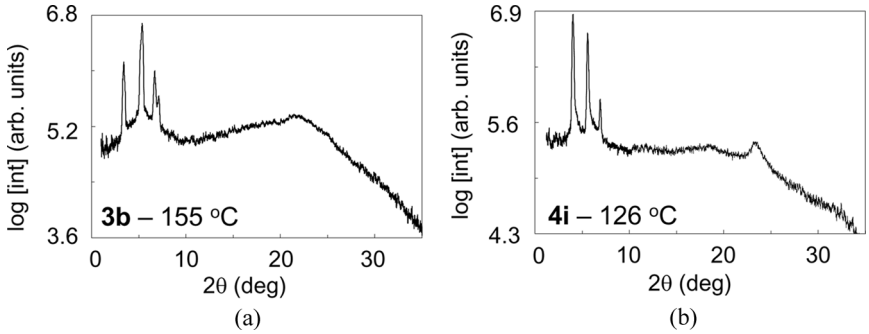

FIGURE 4 XRD intensity vs. 2θ of the twins; (a) compound **3b** at 155°C and (b) compound **4i** at 126°C.

TABLE 2 XRD Data Giving the *hkl* Indexing and Lattice Constants of the Two-Dimensional Lattice

Compound	Temp (°C)	Phase	$d_{exp.}$ (Å)	$d_{cal.}$ (Å)	Miller indices	Lattice constants (Å)
4i	126	Col_r	21.0	21.0	010	$a = 30.5$
			15.2	15.2	200	$b = 21.0$
			12.4	12.3	210	
			4.8			
			3.7			
3d	145	Col_r	27.4	27.4	110	$a = 40.0$
			20.1	20.0	200	$b = 37.5$
			13.8	13.7	220	
			4.7			
			4.0			
3b	155	Col_r	27.8	27.8	110	$a = 35.4$
			17.6	17.7	200	$b = 45.1$
			13.6	13.9	220	
			12.9	11.4		
			5.1			
			4.0			
	145	Col_r	27.9	27.9	110	$a = 34.2$
			17.1	17.1	200	$b = 48.5$
			13.7	14.0	220	
			12.9	11.1		
			5.0			
			3.9			

constants $a = 35.4$ Å and $b = 45.1$ Å (see Table 2). The core-core peak is centered at 4 Å. At low temperature (145°C), the lattice constants were changed to 34.2 Å and 48.5 Å, respectively, and π-π distance decreased to 3.9 Å. The XRD scans of the compound **3d** at 145°C confirmed rectangular columnar phase with lattice constants $a = 40.0$ Å and $b = 37.5$ Å (Table 2). XRD scans taken at 126°C for the compound **4i** (see Fig. 4(b)) showed three sharp reflections in a small angle region. These peaks are indexed to a columnar rectangular lattice with lattice constants $a = 30.5$ Å, $b = 21.0$ Å. In a wide-angle region two diffuse reflections around $2\theta \sim 20^\circ$ appeared and were followed by a fairly sharp peak corresponding to core–core packing at 3.7 Å (Fig. 4(b)). The unit cell of the compound **4i** is much smaller than that of the compound **3b**, although the spacer is shorter in **4i** than **3b**. Thus the rectangular lattice with different lattice constants indicates that distance between two TP moieties and β-substituent plays a significant role in generating supramolecular self-assembled system. Finally, we have to note that molecular packing structure in each column is now known by

the present x-ray analysis; e.g., two triphenelene rings are parallel to each other or not. In the columnar phase, we observed the π-π distance of about 3.7 A in addition to the diffraction due to a rectangular lattice, as mentioned above. In order to obtain more detailed structure information, we have to use well-aligned sample. Then we can tell that the triphenylene core plane is perpendicular to the column axis or not. The determination of the space-filling models based on x-ray analysis using well-aligned samples is our future problems.

Discussion

Based on a previous report [33] and the present results, we discuss the structure and mesogenic property of two TP entities linked with one or two $-C\equiv C-$ rigid spacer. The lengths of the central rigid spacer calculated from Chem3D model are 4.19 Å and 6.96 Å for twins **3a** and **4a**, respectively [44]. The molecular configurations of **3** and **4** with hydrogen-terminated chains can be seen in Fig. 5, indicating that the molecules are planar, if interchain steric interaction is negligible. Twins **3** (**a**–**d**) exhibits the Col_r and/or N mesophases, while twin **4d** and previously reported twins (**4a**–**4c**) having the same peripheral alkoxy chains exhibit only N phase [33]. Derivative **3i** exhibited

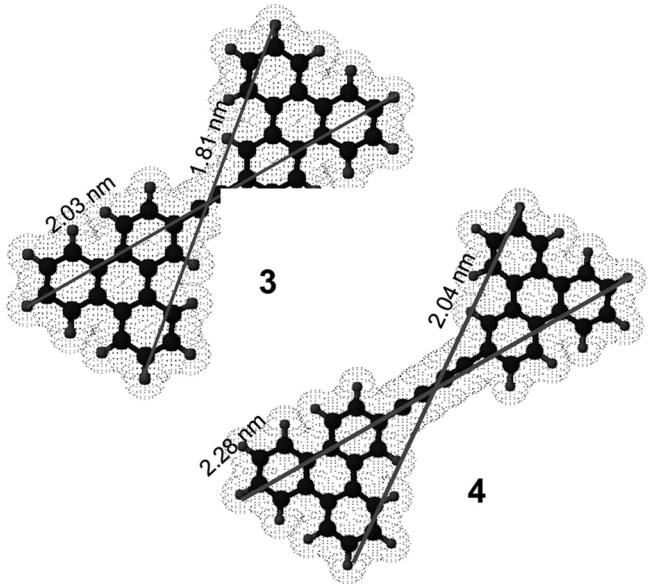

FIGURE 5 Molecular structures and sizes of cores of two twins **3** and **4**. (Aliphatic chains are elimanted for clear view.)

two-dimensional columnar lattices, whereas derivative **4i** exhibited the N phase also. These facts indicate that the β-substituted alkoxy chain and its relative length with respect to the spacer length are very important to realize the N phase. Generally, when the alkoxy tails are increased in length, the melting and isotropic temperatures tend to decrease [45–47]. This is actually the case in **3a**–**3d**. Twin **3h** exhibited the N phase and melting point (m.p.) was 182.8°C, while twin **4h** exhibited M_x mesophase in addition to N, and having m.p. 202.9°C. It is known that on replacing the normal aliphatic chains by the branched aliphatic chains, the transition temperatures often decrease, and the supramolecular self-assembly of DLCs is also affected [45–48].

Interestingly, derivatives **3l** and **4k** show only low-ordered LC phase. **3l** is a kind of combination of **3b** and **3d**. **3l** has only the N phase over a wide temperature range, but the N phase is suppressed particularly in **3d**. **4k** is a kind of combination of **4b** (**3b** in ref. [33]) and **4e**. The mesogenic property of **4k** is much similar to **4b**; both show the wide N temperature range but no Col phase. In contrast, **4e** did not show any mesogenic phase (Table 1). These facts indicate that longer β-substituted alkoxy chain with respect to the spacer length suppress the emergence of the mesogenic phases. The N phase range of **4k** is much lower than that of **4b** by 80°C, which is caused by longer alkoxy chains except for β-substituted one. Based on these results, we can conclude that β-substitution also has vital influence on the molecular self-assembly that donates the molecular orientational and positional order.

It should be worth mentioning here that all the derivatives of twin **3** aligned homeotropically but gave birefringent texture on shearing in the N phase. However, it lost the birefringent texture and went back to dark field of view with time. This phenomenon suggests that the shearing makes the twin linkage direction align along the shearing direction, bringing about the second director, the linkage direction, in addition to the first director, TP plane normal direction, resulting in the biaxial N phase, as illustrated in Fig. 1. The orientational order of the linkage relaxes with time, so that the second director disappears, resulting in the uniaxial N phase. In the case of twin **4**, such an effect was not observed. Further, the enthalpy of N-I or I-N transition is less than $0.5\,Jg^{-1}$ for the twins **3** (symmetrical) whereas the enthalpy is greater than $0.5\,Jg^{-1}$ for twins **4**. This indicates that the fluidity of the N phase is also affected by the length of the rigid spacer. TP entities connected with long flexible spacer exhibits the Col_h mesophase and glassy state while non-mesogenic behavior of twins having short flexible are reported [22]. This could be the reason why compound **5** is non-mesogenic.

3. EXPERIMENTAL

General Information

Materials: Commercially available chemicals and solvents were obtained from commercial suppliers and were used without further purification. The THF and Et_3N were distilled over sodium and potassium hydroxide, respectively, under anhydrous conditions prior to use. Unless otherwise noted, reagents were obtained commercially and were used without any purification.

Techniques: Column chromatographic (CC) separations were performed using silica gel (70–230 and 200–400 mesh) at atmospheric pressure. Analytical thin-layer chromatography (TLC) was performed on aluminum sheets precoated with silica gel (Merck, Kieselgel 60, F_{254}). Mass spectra were recorded on a JEOL JMS-600H spectrometer in FAB^+ mode using 3-nitrobenzylalcohol (NBA) matrix. Elemental analyses were recorded on a EUROVECTOR 3000 series using acetanilide, as standard. ^1H and ^{13}C NMR spectra were recorded on a 200 (^1H) or 400 MHz (^1H, and ^{13}C) machine (Bruker) in $CDCl_3$. All chemical shifts are reported in parts per million downfield from internal tetramethylsilane $CDCl_3$ ($\delta_H = 7.26$, $\delta_C = 77.0$), and the J values are given in Hz.

Liquid-crystalline properties: Transition temperatures were measured using differential scanning calorimetry (DSC-7 Perkin-Elmer). Peak temperatures observed in the heating and cooling runs at the rate of $5^\circ C\ min^{-1}$ are reported. A polarizing optical microscope Leica DMLP equipped with a Mettler FP82HT hot stage and a central processor were used for visual observations. The Leica DFC 320 digital camera was used to get the still images of textures. X-ray studies were performed using an image plate detector (MAC Science DIP1030). Unoriented samples contained in sealed Lindemann glass capillaries were irradiated with Cu K_z rays obtained from a sealed-tube generator (Enraf-Nonius FR 590) in conjunction with double mirror focusing optics.

General Procedures for the Preparation of Protected Acetylene 1(a–j, k)

A mixture of 2-bromopentakis(alkoxy)triphenylene (1 mmol), $Pd[Cl_2P(Ph_3)_2]$ (0.5 mmol), CuI (0.5 mmol), PPh_3 (0.1 mmol), and 2-methyl-3-butyne-2-ol (2 mmol) in THF (10 ml) and Et_3N (15 ml) was heated at $80^\circ C$ for 24 h. After cooling to room temperature (RT), solid was filtered via Celite. The filtrate was concentrated and was purified by CC over SiO_2 as white solid.

1(a): IR (KBr): 2957, 2932, 2871, 2220, 1616, 1517, 1458, 1435, 1387, 1262, 1187, 1170, 1072, 1034 cm^{-1}; δ_H 8.46 (s, 1 H), 7.87 (d, $J = 3.6$, 2 H), 7.8 (s, 2 H), 7.73 (s, 1 H), 4.24–4.2 (m, 10 H), 2.17 (s, 1 H), 1.96–189 (m, 10 H), 1.71–1.51 (m, 16 H), 1.08–1.0 (m,15 H); MS (FAB^+): m/z (%) 670 (100) [M^+], 671 (59), 672 (19), 674 (5).

1(b): IR (KBr): 3434, 2930, 2857, 2250, 1613, 1517, 1466, 1433, 1387, 1264, 1174, 1052, 1073 cm^{-1}; δ_H 8.46 (s, 1 H), 7.85 (d, $J = 7.8$, 2 H), 7.80 (s, 2 H), 7.73 (s, 1 H), 4.28–4.18 (m, 10 H), 2.17 (s, 1 H), 2.0–1.9 (m, 10 H), 1.72 (s, 6H), 1.65–1.40 (m, 20 H), 1.1–0.95 (m, 15 H); MS (FAB^+); m/z (%)739 (11), 740 (15) [M^+], 741 (100), 742.29 (58), 743 (22), 744 (6).

1(c): IR (KBr): 2919, 2853, 1613, 1507, 1466, 1431, 1385, 1262, 1173, 1048 cm^{-1}. δ_H 8.47 (s, 1 H), 7.86 (d, $J = 3.2$, 2 H), 7.8 (s, 2 H), 7.74 (s, 1 H), 4.23–4.22 (m, 10 H), 2.14 (s, 1 H), 1.93–1.9 (m, 10 H), 1.71 (s, 6 H), 1.55 (m, 10 H), 1.40 (m, 20 H), 0.95 (t, $J = 6.8$, 15 H); MS (FAB^+) m/z (%): 809 (15), 810 (17%), 811 (100) [M^+], 812 (61), 813 (25).

1(d): IR(KBr): 2922, 2849, 1613, 1510, 1466, 1432, 1385, 1263, 1174, 1064 cm^{-1}; δ_H 8.46 (s, 1 H), 7.85 (d, $J = 6.9$, 2 H), 7.79 (s, 2 H), 7.74 (s, 1 H), 4.27–4.19 (m, 10 H), 2.2-(s, 1 H), 2.0–1.89 (m, 10 H), 1.72 (s, 6 H), 1.66–1.5 (m, 10 H), 1.48–1.28 (m, 30 H), 0.9 (t, $J = 6.14$, 15 H); MS (FAB^+) m/z (%): 879 (20), 880 (21) [M^+], 881 (100), 882 (66), 883 (29).

1(e): IR(KBr): 3523, 2920, 2849, 1613, 1517, 1466, 1432, 1385, 1264, 1175, 1067, 1027 cm^{-1}; δ_H 8.47 (s, 1 H, Ar), 7.86 (d, $J = 6.7$, 2 H), 7.8 (s, 2 H), 7.74 (s, 1 H), 4.26–4.2 (m, 10 H), 2.17 (s, 1 H), 1.99–1.90 (m, 10 H), 1.72 (s, 6 H), 1.69–1.27 (m, 50 H), 0.89 (t, $J = 6.7$, 15 H); MS (FAB^+) m/z (%): 950 (58) [M^+], 951 (46), 952 (16).

1(f): IR(KBr): 2953, 2925, 2868, 1612, 1508, 1466, 1432, 1383, 1262, 1188, 1169, 1048 cm^{-1}; δ_H 8.48 (s, 1 H), 7.87 (s, 1 H), 7.81 (s, 2 H), 7.76 (s, 2 H), 4.27 (m, 10 H), 2.01 (m, 6 H), 1.97–1.77 (m, 16 H), 1.61–148 (m, 10 H), 1.37–1.19 (m, 40 H), 0.89 (d, $J = 6.6$, 30 H); MS (FAB^+) m/z (%): 1092 (64) [$M^+ + 1H$], 1095 (32), 1096 (30).

1(g): IR(KBr): 2953, 2925, 2855, 1613, 1516, 1465, 1430, 1388, 1264, 1177, 1051 cm^{-1}; δ_H 8.51 (s, 1 H), 8.38 (d, $J = 8.7$, 1 H), 7.95 (s, 2 H), 7.81 (s, 2 H), 7.57 (dd, $J = 7$, 1 H), 4.26–4.20 (m, 8 H), 1.99–1.92 (m, 8 H), 1.71 (m, 6 H), 1.68–1.0 (m, 16 H), 0.97 (t, $J = 4.6$, 12 H); MS (FAB^+) m/z (%): 651 (100), 652 (50), 653 (89), 654 (50) [M^+].

1(h): IR(KBr): 3528, 2952, 2927, 2858, 1612, 1541, 1511, 1464, 1450, 1426, 1388, 1265, 1176, 1053 cm^{-1}; δ_H 8.46 (s, 1 H), 7.86 (s, 2 H), 7.79 (s, 2 H), 7.73 (s, 1 H), 4.27–4.22 (m, 8 H), 4.09 (s, 3 H), 2.26 (s, 1 H), 1.95–1.93 (m, 8 H), 1.73 (s, 6 H), 1.57–1.37 (m, 16 H), 0.98 (t, $J = 6.7$, 12 H);. MS (FAB^+) m/z (%): 683 (10), 684 (13) [M^+], 685 (100), 686 (60), 687 (20).

1(i): IR (KBr): 2955, 2929, 2870, 1616, 1508, 1432, 1384, 1263, 1170, 1053 cm^{-1}; δ_H 8.46 (s, 1 H), 7.85 (d, $J = 4.3$, 2 H), 7.8 (s, 2 H), 7.74 (s, 1 H), 4.32–4.19 (m, 10 H), 2.18 (s, 1 H), 2.2–1.9 (m, 10 H), 1.71 (s, 6 H), 1.62–1.3 (m, 21 H), 1.23–1.17 (m, 3 H), 1.18 (d, $J = 7.16$, 3 H), 1.02–0.93 (m, 12 H), 0.87(d, $J = 6.6$, 6 H); MS (FAB^+) m/z (%): 811 (100) [M^+], 812 (59), 813 (28).

1(j): IR (KBr): 3525, 2954, 2927, 2857, 1613, 1516, 1465, 1433, 1387, 1264, 1174, 1052 cm^{-1}; δ_H 8.47 (s, 1 H), 7.87 (s, 2 H), 7.8 (s, 2 H), 7.73 (s, 1 H), 4.4.27–4.21 (m, 8 H), 4.16–4.12 (m, 2 H), 2.12 (s, 1 H), 1.99–1.93 (m, 9 H), 1.71(s, 6 H), 1.66–1.37 (m, 27 H), 1.02 (m, 15 H); MS (FAB^+) m/z (%): 780 (12), 781 (16), 782 (100) [M+], 783 (63), 784 (22).

1(k): IR (KBr): 2924, 2855, 2363, 2344, 1616, 1508, 1436, 1388, 1264, 1170, 1045 cm^{-1}; δ_H 8.47 (s, 1 H), 7.86 (d, $J = 4$, 2 H), 7.80 (s, 2 H), 7.74 (s, 1 H), 4.24–4.03 (m, 10 H), 2.12 (s, 1 H), 1.94–1.72 (m, 10 H), 1.71 (s, 6 H), 1.57–1.31 (m, 44 H), 1.0–0.86 (m, 15 H); MS (FAB^+) m/z (%): 910 (100) [$M^+ + 1$ H], 911 (66), 912 (32).

General Procedure for the Preparation of Free Acetylene 2(a–f, h–k)

The protected acetylene (**1**) (1 mmol) was heated under reflex with KOH (2 mmol) in toluene under anhydrous conditions for 2 h. The reaction mixture was cooled and poured into a mixture of conc. HCl and ice (pH$\sim$7). The crude product was extracted into (3×100 ml) diethyl ether and was dried over anhydrous sodium sulphate. The solvent was removed, the crude product was purified by CC over Al_2O_3 eluted 1% (v/v) ethyl acetate/hexane to yield (70–90%) a solid or semisolid.

2(a): IR (KBr): 3313, 2956, 2871, 2100, 1612, 1517, 1435, 1394, 1262, 1194, 1171, 1046 cm^{-1}; UV-vis λ_{max} (ε_{max}): 283 (1.19), 336 (0.14) nm (10^5 L mol^{-1} cm^{-1}); δ_H 8.55 (s, 1 H), 7.85 (s, 2 H), 7.79 (s, 2 H), 7.76 (s, 1 H), 4.31–4.20 (m, 10 H), 3.39 (s, 1 H), 1.99–1.86 (m, 10 H), 1.69–1.51 (m, 10 H),1.04 (t, $J = 7.3$, 15 H); MS (FAB^+); m/z (%):610 (7), 611(11), 612 (100) [M^+], 613 (65), 614 (23), 615 (9.6).

2(b)[1]: IR(KBr): 3314, 2955, 1616, 1540, 1507, 1435, 1387, 1262, 1170, 1040 cm^{-1}; UV-VIS λ_{max} (ε_{max}): 283 (1.2) nm (10^5 L mol^{-1} cm^{-1}); δ_H 8.56 (s, 1 H), 7.85 (d, $J = 2.8$, 2 H), 7.79 (s, 2 H), 7.76 (s, 1 H), 4.31–4.2 (m, 10 H), 3.4 (s, 1 H), 1.98–1.92 (m, 10 H), 1.61–1.41 (m, 20 H), 0.97 (t, $J = 7$, 15 H); MS (FAB^+) m/z (%):681 (13), 682 (13), 683 (100) [M^+], 684 (79), 685 (34), 686 (14).

2(c): IR (KBr): 3313, 2929, 2858, 1611, 1540, 1508, 1432, 1388, 1262, 1171, 1040 cm^{-1}; UV-vis λ_{max} (ε_{max}): 283 (0.73), 335 (0.9) nm (10^5 L mol^{-1} cm^{-1}); δ_H 8.55 (s, 1 H), 7.85 (s, 2 H), 7.79 (s, 2 H), 7.76

(s, 1 H), 4.30–4.19 (m, 10 H), 3.39 (s, 1 H), 1.97–1.91 (m, 10 H), 1.57–1.4 (m, 30 H), 0.97 (t, $J = 7$, 15 H); MS (FAB^+) m/z (%): 753 (100) [M^+], 754 (76), 755 (32).

2(d): IR (KBr): 3313, 2925, 2855, 1611, 1508, 1432, 1387, 1262, 1170, 1042 cm^{-1}; UV-vis λ_{max} (ε_{max}): 283 (1.14), 336 (0.14) nm (10^5 L mol^{-1} cm^{-1}); δ_H 8.56 (s, 1 H), 7.86 (s, 2 H), 7.8 (s, 2 H), 7.77 (s, 1 H), 4.30–4.19 (m, 10 H), 3.39 (s, 1 H), 1.97–1.91 (m, 10 H), 1.55–1.36 (m, 40 H), 0.91 (t, $J = 6.1$, 15 H); MS (FAB^+); m/z (%):823 (100) [M^+], 824 (78), 825 (35).

2(e): IR (KBr): 3313, 2924, 2854, 1616, 1540, 1508, 1435, 1386, 1263, 1170, 1044 cm^{-1}; UV-vis λ_{max} (ε_{max}): 283 (1.33), 335 (0.16) nm (10^5 L mol^{-1} cm^{-1}); δ_H 8.56 (s, 1 H, Ar), 7.86 (s, 2 H), 7.80 (s, 2 H), 7.77 (s, 1 H), 4.30–4.19 (m, 10 H), 3.39 (s, 1 H), 1.97–1.91 (m, 10 H), 1.55–1.31 (m, 50 H), 0.89–0.87 (m, 15 H); MS (FAB^+) m/z (%): 892 (100) [M^+], 893 (80).

2(f): IR (KBr): 3313, 2953, 2925, 2868, 1611, 1508, 1458, 1435, 1383, 1261, 1169, 1040 cm^{-1}; UV-vis λ_{max} (ε_{max}): 284 (1.15) 337 (0.13) nm (10^5 L mol^{-1} cm^{-1}); δ_H 8.57 (s, 1 H), 7.87 (s, 2 H), 7.81 (s, 2 H), 7.78 (s, 1 H), 4.29–4.26 (m, 10 H), 3.39 (s, 1 H), 1.98 (m, 5 H), 1.77 (m, 10 H), 1.61–1.19 (m, 35 H), 1.02 (d, $J = 5.8$, 15 H), 0.87 (d, $J = 6.6$, 30 H); MS (FAB^+) m/z (%):1028 (10), 1034 (100) [$M^+ + 2H$], 1036 (45).

2(h): IR (KBr): 3290, 2953, 2857, 1612, 1508, 1465, 1425, 1386, 1263, 1173, 1053 cm^{-1}; UV-vis λ_{max} (ε_{max}): 283 (1.23), 337 (0.16) nm (10^5 L mol^{-1} cm^{-1}); δ_H 8.61 (s, 1 H), 7.91 (s, 2 H), 7.85 (s, 2 H), 7.82 (s, 1 H), 4.32–4.22 (m, 8 H), 4.18 (s, 3 H), 3.48 (s, 1 H), 2.03–1.96 (m, 8 H), 1.68–1.3 (m, 16 H), 1.05–0.9 (m, 12 H); MS (FAB^+); m/z (%):627 (100) [M^+].

2(i): IR (KBr): 3313, 2955, 1615, 1507, 1457, 1431, 1387, 1262, 1170, 1039 cm^{-1}; UV-vis λ_{max} (ε_{max}): 283 (1.13), 355 (0.14) nm (10^5 L mol^{-1} cm^{-1}); δ_H 8.55 (s, 1 H), 7.86 (s, 2 H), 7.80 (d, $J = 2.5$, 2 H), 7.77 (s, 1 H), 4.34–4.21 (m, 10 H), 3.37 (s, 1 H), 2.03–1.92 (m, 10 H), 1.8–1.73 (m, 2 H), 1.59–1.29 (m, 18 H), 1.27–1.2 (m, 4 H), 1.04 (d, $J = 6.4$, 3 H), 0.97 (m, 12 H), 0.88 (d, $J = 6.6$, 6 H); MS (FAB^+); m/z (%):753 (100) [M^+].

2(j): IR (KBr): 3310, 2957, 2932, 2872, 1616, 1507, 1435, 1385, 1262, 1170, 1042 cm^{-1}; UV-vis λ_{max}(ε_{max}): 283 (0.67) nm (10^5 L mol^{-1} cm^{-1}); δ_H 8.48 (s, 1 H, Ar), 7.79 (s, 2 H), 7.73 (s, 2 H), 7.69 (s, 1 H), 4.19–4.14 (m, 8 H), 4.0 (d, $J = 5.6$, 2 H), 3.30 (s, 1 H), 1.89–1.81 (m, 11 H), 1.60–1.18 (m, 22 H), 0.97–0.84 (m, 18 H); MS (FAB^+); m/z (%):725 (23) [M^+], 726 (16).

2(k): IR (KBr): 3313, 2957, 2925, 2854, 2364, 2344, 1610, 1508, 1431, 1388, 1263, 1170, 1043 cm^{-1}; UV-vis λ_{max} (ε_{max}): 283 (1.11), 336 (0.14) nm (10^5 L mol^{-1} cm^{-1}); δ_H 8.56 (s, 1 H), 7.83 (d, $J = 2.8$,

2 H), 7.8 (s, 2 H), 7.77 (s, 1 H), 4.24–4.22 (m, 10 H), 3.4 (s, 1 H), 1.94 (m, 10 H), 1.56–1.32 (m, 44 H), 0.98 (t, $J = 7.2$, 3 H), 0.89 (t, $J = 6.5$, 12 H); MS (FAB$^+$) m/z (%): 852 (18) [M$^+ + 2$ H], 853 (78), 854 (69), 857 (44).

General Procedure for the Preparation of Ethynyl-Bridge Twin 3(a–d, h–i, l)

2-Iodopentakis(alkoxy)triphenylene (1.1 mmol), 2-ethynylpentakis-(alkoxy)TP (1 mmol), Pd[$Cl_2P(Ph_3)_2$] (0.05 mmol, 5%), CuI (0.05 mmol, 5%), and $P(Ph)_3$ (0.1 mmol) were placed into a flame-dried round bottom flask and mixture was deoxygenate. 15 ml Et_3N as a base and 5 ml THF were added under the anhydrous condition. The mixture was heated under reflex in an atmosphere of dry Argon for 36 h, after which it was cooled and filtered via Celite. The filtrate was concentrated and purified by column chromatography (X 3) over silica gel using hexane/dichloromethane as eluent to give desired ethynyl-bridge twin (yield 30%) as a solid. Finally, recrystallization from diethyl ether-ethyl alcohol to afford a solid.

(3a): IR (KBr): 2957, 2932, 2870, 1610, 1508, 1431, 1388, 1262, 1173, 1068, 1043 cm^{-1}; UV-vis (CH_2Cl_2) λ_{max} (ε_{max}) 263 (0.84), 290 (1.15), 377 (0.53) nm (10^5 L mol^{-1} cm^{-1}); δ_H 8.70 (s, 2 H), 7.86 (m, 10 H), 4.30 (m, 20 H), 1.97 (m, 20 H), 1.67 (m, 20 H), 1.05 (t, $J = 7.3$ Hz, 30 H); δ_C 158.5, 157.6, 150.4, 150.2, 149.7, 149.1, 131.0, 130.3, 129.9, 128.6, 125.6, 123.6, 123.3, 123.0, 122.8, 113.2, 111.3, 108.2, 107.7, 107.0, 106.3, 105.2, 104.8, 90.7, 79.8, 69.6, 69.2, 69.0, 31.5, 19.4, 13.9; MS (FAB$^+$): m/z (%) = 1200.6 (13) [M$^+$], 1202 (10). C_{78} $H_{102}O_{10}$ (1198.75): calcd. C 78.09, H 8.57; found C 78.28, H 8.27.

(3b): IR (KBr): 2954, 2930, 2870, 1654, 1616, 1508, 1458, 1437, 1387, 1263, 1175, 1051 cm^{-1}; UV-vis λ_{max} (ε_{max}): 263 (0.88), 287 (1.15), 366 (0.51) nm (10^5 L mol^{-1} cm^{-1}); δ_H: 8.70 (s, 2 H), 7.96 (s, 2 H), 7.89 (s, 2 H), 7.84 (s, 6 H), 4.41 (t, $J = 6.6$, 4 H), 4.32–4.22 (m, 16 H), 2.05–1.95 (m, 20 H), 1.68–1.45 (m, 40 H), 1.0–0.91 (m, 30 H); δ_C:157.6, 150.2, 149.6, 149.0, 130.3, 128.6, 125.3, 123.6, 123.0, 113.2, 108.2, 170.7, 107.2, 106.8, 105.3, 90.7, 69.9, 69.6, 69.4, 29.6, 28.3, 22.5, 14.0; MS (FAB$^+$): m/z (%) = 1339.5 (11) [M$^+$], 1342 (3). C_{88} $H_{122}O_{10}$ (1339.9): calcd. C 78.88, H 9.18; found C 79.21, H 8.82.

(3c): IR (KBr): 2952, 2926, 2857, 1617, 1512, 1466, 1431, 1387, 1262, 1173, 1049 cm^{-1}; UV-vis λ_{max} (ε_{max}) 263 (0.75), 287 (1), 366 (0.42) nm (10^5 L mol^{-1} cm^{-1}); δ_H 8.77 (s, 2 H), 8.02 (s, 2 H), 7.97 (s, 2 H), 7.90 (s, 6 H), 4.42 (t, $J = 6.6$, 4 H), 4.30–4.28 (m, 16 H), 2.12–1.97 (m, 20 H), 1.73–1.62 (m, 20 H), 1.51–1.36 (m, 40 H), 1.02–.96 (m, 24 H), 0.90 (t, $J = 7.2$, 6 H); δ_C 157.7, 150.3, 149.6, 149.0, 130.3, 128.6, 127.5, 125.4, 123.7, 123.2, 123.1, 121.2, 113.3, 108.3, 107.8, 107.2, 106.8, 105.3,

90.7, 70.0, 69.6, 69.4, 34.1, 33.8, 33.3, 32.0, 31.7, 29.5, 25.8, 22.6, 14.0; MS (FAB$^+$): m/z (%) = 1482 (17) [M^{+2}], 1484 (13). $C_{98}H_{142}O_{10}$ (1479.06): calcd. C 79.52, H 9.67; found C 78.93, H 9.73.

(3d): IR (KBr): 2952, 2924, 2852, 1616, 1508, 1465, 1432, 1387, 1263, 1173, 1066 cm^{-1}; UV-vis λ_{max} (ε_{max}) 263 (0.73), 287 (0.98), 366 (0.41) nm (10^5 L mol^{-1} cm^{-1}); δ_H 8.70 (s, 2 H), 7.95 (s, 2 H), 7.91 (s, 2 H), 7.85 (s, 2 H), 7.83 (s, 4 H), 4.36 (t, J = 6.8, 4 H), 4.27–4.22 (m, 16 H), 2.0–1.91 (m, 20 H), 1.67–1.54 (m, 20 H), 1.40–1.22 (m, 60 H), 0.93–0.87 (m, 24 H), 0.78 (t, J = 6.8, 6 H); δ_C 157.7, 150.3, 149.6, 149.1, 141.7, 131.3, 130.3, 128.6, 125.4, 123.7, 123.2, 123.1, 121.9, 113.3, 108.3, 107.9, 107.3, 106.8, 105.4, 91.8, 90.7, 70.0, 69.7, 69.5, 69.4, 65.9, 31.8, 29.6, 29.1, 26.1, 22.6, 19.4, 14.0. MS (FAB$^+$): m/z (%) = 1619 (8), 1620.0 (8) [M$^+$]. $C_{108}H_{162}O_{10}$ (1619.22): calcd. C 80.05, H 10.08; found C 80.38, H 10.11.

(3h): IR (KBr thin film): 2957, 2932, 2860, 1615, 1508, 1466, 1430, 1263, 1172, 1050 cm^{-1}; UV-vis λ_{max} (ε_{max}) 263 (0.76), 286 (1.09), 366 (0.42) nm (10^5 L mol^{-1} cm^{-1}); δ_H 8.74 (s, 2 H), 7.97 (s, 2 H), 7.92 (s, 2 H), 7.83 (s, 6 H), 4.29–4.15 (m, 22 H), 2.0–1.90 (m, 16 H), 1.65–1.37 (m, 32 H), 0.98 (t, J = 7.0, 24 H); δ_C 158.0, 150.3, 149.6, 149.1, 149.0, 130.4, 128.8, 125.4, 123.6, 123.2, 123.0, 112.4, 108.2, 107.7, 107.2, 106.9, 103.4, 90.7, 70.0, 69.6, 69.5, 56.3, 29.2, 28.4, 22.5, 14.0; MS (FAB$^+$): m/z (%) = 1227 (100) [M$^+$]. $C_{80}H_{106}O_{10}$ (1226.78): calcd. C 78.27, H 8.70; found C 77.81, H 9.0.

(3i): IR (KBr thin film): 2954, 2930, 2869, 1616, 1508, 1431, 1387, 1263, 1174, 1052 cm^{-1}; UV-vis λ_{max} (ε_{max}) 263 (0.85), 287 (1.16), 365 (0.48) nm (10^5 L mol^{-1} cm^{-1}); δ_H 8.69 (s, 2 H), 7.96 (s, 2 H), 7.91 (s, 2 H), 7.89 (s, 2 H), 7.88 (s, 4 H), 4.39–4.22 (m, 20 H), 2.11–1.83 (m, 24 H), 1.59–1.2 (m, 44 H), 1.08(d, J = 8.9, 6 H), 0.98 (m, 24 H), 0.73 (dd, J = 5.8, 12 H); δ_C 150.3, 149.0, 130.3, 128.6, 123.0, 116.5, 108.3, 107.8, 107.3, 106.9, 105.2, 90.7, 70.0, 69.7, 69.5, 68.2, 68.0, 39.2, 37.6, 36.4, 30.3, 29.2, 28.4, 27.9, 24.8, 22.5, 20.0, 14.2, 14.0; (FAB$^+$): m/z (%) = 1479 (100) [M$^-$]. $C_{98}H_{142}O_{10}$ (1479.06): calcd. C 79.52, H 9.67; found C 79.40, H 9.89.

(3l): IR (KBr thin film): 2955, 2929, 2857, 1611, 1508, 1466, 1436, 1387, 1263, 1173, 1042 cm^{-1}; UV-vis λ_{max} (ε_{max}) 263 (0.82), 287 (1.09), 366 (0.46) nm (10^5 L mol^{-1} cm^{-1}); δ_H 8.70 (s, 2 H), 7.96 (s, 2 H), 7.91 (s, 2 H), 7.85 (s, 2 H), 7.83 (s, 4 H), 4.38 (t, J = 6.6, 4 H), 4.24 (m, 16 H), 2.07–1.9 (m, 20 H), 1.67–1.55 (m, 20 H), 1.49–1.25 (m, 40 H), 1.0–0.87 (m, 24 H), 0.77 (t, J = 6.8, 6 H); δ_C 157.7, 149.6, 149.0, 130.3, 128.6, 125.4, 123.6, 123.2, 123.0, 108.1, 107.7, 107.1, 106.8, 105.3, 70.0, 69.6, 69.4, 31.8, 29.5, 29.2, 28.4, 26.1, 22.5, 15.2, 14.0; MS (FAB$^+$): m/z (%) = 1481 [M^{+1}], (66), 1483 (100), 1487 (38), 1496 (54). $C_{98}H_{142}O_{10}$ (1479.06): calcd. C 79.52, H 9.67; found C 79.24, H 9.59.

General Procedure for the Preparation of Butadiynyl-Bridge Twin 4(d–k)

Copper (II) acetate monohydrated (4 mmol) was added to a solution of 2-ethynylpentakis(alkoxy)triphenylene **1** (1 mmol) in pyridine (4 mL), THF (4 mL), and methanol (1 mL), and mixture was heated under an reflux in an argon atmosphere for 24 h, after which it was cooled, insoluble solids were removed by filtration. The filtrate was dried and evaporated under reduced pressure to leave a brown solid, which was purified by column chromatography on aluminum oxide using EtOAc/hexane as eluent to give the butynyl-bridge twin **4** (yield 80%) as a yellow solid. Finally, it was purified by recrystallization from diethyl ether/ethyl alcohol to afford a bright yellow solid.

4(d): IR (KBr,): 2958, 2926, 2855, 1607, 1508, 1429, 1386, 1263, 1172, 1042 cm^{-1}; UV-vis λ_{max} (ε_{max}) 263 (1.04), 290 (1.53), 377 (0.69), 408 (0.52) nm (10^5 L mol^{-1} cm^{-1}); δ_H 8.60 (s, 2 H), 7.88 (s, 2 H), 7.86 (s, 2 H), 7.80 (s, 4 H), 7.78 (s, 2 H), 4.30 (t, $J = 6.5$, 4 H), 4.26–4.21 (m, 16 H), 2.0–1.94 (m, 20 H), 1.67–1.25 (m, 80 H), 0.91–0.89 (m, 30 H); δ_C 158.5, 150.5, 149.7, 149.0, 131.0, 129.9, 125.7, 123.4, 123.1, 122.8, 111.5, 108.4, 107.8, 107.1, 106.4, 105.0, 70.0, 69.6, 69.5, 69.4, 31.9, 29.6, 29.5, 29.3, 29.2, 26.2, 22.6, 14.0; MS (FAB^+): m/z (%) = 1645 (6) [M^{+1}]. $C_{110}H_{162}O_{10}$ (1643.22): calcd. C 80.34, H 9.63; found C 79.94, H 9.59.

4(e): IR (KBr): 2958, 2923, 2853, 1609, 1518, 1432, 1389, 1262, 1174, 1044 cm^{-1}; UV-vis λ_{max} (ε_{max}): 263 (1.07), 290 (1.7), 377 (0.7), 408 (0.54) nm (10^5 L mol^{-1} cm^{-1}); δ_H 8.65 (s, 2 H), 7.88 (s, 2 H), 7.87 (s, 2 H), 7.81 (s, 4 H), 7.78 (s, 2 H), 4.33–4.23 (m, 20 H), 1.97–1.94 (m, 20 H), 1.58–1.32 (m, 100 H), 0.90–0.85 (m, 30 H); δ_C 150.5, 149.8, 149.0, 131.0, 129.9, 125.7, 123.1, 122.8, 108.4, 107.9, 107.1, 106.4, 104.0, 70.0, 69.6, 69.5, 31.8, 29.4, 29.3, 26.2, 22.6, 14.0; MS (FAB^+): m/z (%) = 1782 (5), 1784 (3) [M^+], 1786 (2). $C_{120}H_{182}O_{10}$ (1783.37): calcd. C 80.76, H 10.28; found C 79.24, H 9.59.

4(f): UV-vis λ_{max} (ε_{max}): 264 (0.69), 290 (0.97), 377 (0.49), 408 (0.31) nm (10^5 L mol^{-1} cm^{-1}); δ_H 8.65 (s, 2 H), 7.88 (s, 2 H), 7.82 (s, 4 H), 7.79 (s, 4 H), 4.25 (m, 20 H), 2.02 (m, 10 H), 1.78 (m, 20 H), 1.55 (m, 20 H), 1.4–1.0 (m, 50 H), 1.03 (m, 30 H), 0.9 (m, 60 H); δ_C 150.4, 149.1, 131.0, 129.9, 125.6, 123.3, 122.8, 111.5, 108.2, 107.6, 107.0, 106.3, 104.8, 68.3, 67.9, 67.7, 39.3, 37.5, 36.5, 36.2, 34.7, 33.9, 30.1, 29.6, 29.4, 28.0, 24.8, 22.7, 22.6, 19.8, 19.2, and 11.3; MS (FAB^+): m/z (%) = 2060 (22), 2075 (100), 2089 (21) [M^{+Na}], 2094 (27). $C_{140}H_{222}O_{10}$ (2063.69): calcd. C 81.42, H 10.83; found C 81.04, H 10.44.

4(g): IR (KBr, cm^{-1}): 2928, 2366, 2344, 1425, 1171, 1052; UV-VIS λ_{max} (nm): 289, 378; $\varepsilon_{max} = 2.06 \times 10^5$; δ_H 8.69 (s, 2 H), 8.42 (d, 2 H,

$J = 9$), 7.96 (s, 4 H), 7.81(s, 4 H), 7.7(d, 4 H, J = 9.7), 4.28–4.2 (m, 16 H), 1.99–1.93(m, 16 H), 1.54–1.01 (m, 32 H), 0.99–0.94 (m, 24 H); δ_C 150, 149.7, 149.2, 129.3, 128.9, 128.7, 127.6, 124.7, 124.2, 123.0, 122.8, 122.7, 118.6, 107.0, 106.8, 106.7, 106.4, 82.9, 74.3, 69.6, 69.5, 69.2, 29.0, 28.3, 22.5, and 14.0; MS (FAB^+): m/z (%) = 1191 (2) [M^+]. $C_{80}H_{102}O_8$ (1190.76): calcd. C 80.63, H 8.63; found C 81.0, H 8.51.

4(h): IR (KBr): 2928, 2366, 2344, 1465, 1458, 1425, 1388, 1264, 1174, 1054 cm^{-1}; UV-VIS λ_{max} (ε_{max}): 264 (1.56), 289 (2.06), 378 (0.91) nm (10^5 L mol^{-1} cm^{-1}); δ_H 8.60 (s, 2 H), 7.84 (s, 4 H), 7.77 (s, 4 H), 7.72 (s, 2 H), 4.28–4.20 (m, 16 H), 4.14 (s, 6 H), 2.0–1.88 (m, 16 H), 1.64–1.37 (m, 32 H), 1.0–0.94 (m, 24 H); δ_C 159.5, 151.2, 150.3, 150.0, 149.8, 149.6, 131.6, 130.7, 126.3, 123.9, 123.7, 123.6, 123.4, 111.4, 108.9, 108.3, 107.6, 106.9, 103.9, 70.6, 70.2, 70.0, 56.8, 30.3, 29.8, 29.0, 23.2, 14.7; MS (FAB^+): m/z (%) = 1250.6 (51) [M^+]. $C_{82}H_{106}O_{10}$(1250.78): calcd. C 78.68, H 8.54; found C 78.8, H 8.39.

4(i): IR (KBr): 2954, 2869, 1608, 1508, 1466, 1429, 1385, 1312, 1263, 1171, 1051 cm^{-1}; UV-VIS λ_{max} (ε_{max}): 263 (0.65), 289 (0.93), 377 (0.40), nm (10^5 L mol^{-1} cm^{-1}); δ_H 8.64 (s, 2 H), 7.88 (s, 2 H), 7.87 (s, 2 H), 7.81 (s, 4 H), 7.79 (s, 2 H), 4.34 (t, $J = 6.9$, 4 H), 4.29–4.20 (m, 16 H), 2.0–1.84 (m, 20 H), 1.61–1.2(m, 48 H), 1.08(d, $J = 6.9$, 6 H), 0.98(t, $J = 6.5$, 24 H), 0.84(d, $J = 6.2$, 12 H); δ_C 158.5, 150.5, 149.7, 149.1, 149.0, 131.0, 130.0, 125.7, 123.4, 123.1, 122.9, 111.5, 108.4, 107.8, 107.1, 106.4, 104.8, 70.0, 69.6, 69.3, 67.8, 39.3, 37.5, 36.2, 30.2, 29.2, 29.1, 28.4, 28.0, 24.8, 22.5, 20.0,14.0; MS (FAB^+): m/z (%) = 1503 (34), 1504 (26) [M^+]. $C_{100}H_{142}O_{10}$ (1503.06): calcd. C 79.85, H 9.52; found C 80.33, H 9.47.

4(j): IR (KBr,): 2954, 2860, 1608, 1508, 1466, 1430, 1388, 1312, 1263, 1173, 1052 cm^{-1}; UV-VIS λ_{max} (ε_{max}): 263 (0.8), 290 (1.2), 377 (0.55), 409 (0.44) nm (10^5 L mol^{-1} cm^{-1}); δ_H 8.64 (s, 2 H), 7.88 (s, 2 H), 7.87 (s, 2 H), 7.8 (s, 4 H), 7.77 (s, 2 H), 4.27–4.24 (m, 16 H), 4.20 (t, $J = 5.4$, 4 H), 2.0–1.94 (m, 18 H), 1.69–1.40 (m, 48 H), 1.06 (t, $J = 7.6$, 6 H), 0.98 (m, 30 H); δ_C 158.7, 150.4, 149.6, 149.0, 148.9, 130.9, 129.7, 125.6, 123.4, 123.0, 122.8, 111.5, 108.4, 107.7, 107.0, 106.4, 104.6, 71.8, 70.0, 69.5, 69.3, 39.5,, 30.8, 29.2, 29.1, 29.0, 28.3, 27.9, 24.2, 23.0, 22.5, 13.9,11.3; MS (FAB^+): m/z (%) = 1447 (10) [M^-]. $C_{96}H_{134}O_{10}$ (1447.00): calcd. C 79.62, H 9.33; found C 79.80, H 9.81.

4(k): IR (KBr,): 2924, 2854, 1608, 1508, 1466, 1430, 1387, 1264, 1173, 1044 cm^{-1}; UV-VIS λ_{max} (ε_{max}): 63 (1.67), 290 (2.33), 37 (1.02) nm (10^5 L mol^{-1} cm^{-1}); δ_H 8.64 (s, 2 H), 7.87 (s, 4 H), 7.78 (s, 6 H), 4.34–4.23 (m, 20 H), 1.98–1.95 (m, 20 H), 1.58–1.31 (m, 88 H), 1.01 (t, $J = 7.0$, 6 H), 0.9 (m, 24 H); δ_C 158.5, 150.5, 149.7, 148.9, 131.0, 129.9, 125.6, 123.3, 123.0, 122.8, 111.4, 108.3, 107.8, 107.0, 106.3,

104.9, 70.0, 69.6, 69.4, 69.3, 31.8, 29.4, 29.3, 28.9, 28.3, 26.2, 22.6, and 14.0. MS (FAB^+): m/z (%) = 1700 (2) [M^+]. $C_{114}H_{170}O_{10}$ (1699.28): calcd. C 80.52, H 10.08; found C 80.42, H 9.5.

Procedure for the Preparation of Compound 5

Compound 4b was dissolved in ethyl acetate and a catalytic amount of Pd/C was added and stirred at RT for 15 h under hydrogen atmosphere. Solid impurities were removed by filtration. The filtrate was dried and evaporated under reduced pressure to leave a colorless solid, which was purified by column chromatography on SiO_2 using EtOAc/hexane as eluent to give the target molecules 5 (yield 95%) as a white solid. Finally, it was purified by recrystallisation from ethyl alcohol to afford a white solid.

δ_H 8.17 (s, 2 H), 7.89 (d, $J = 6.44$, 4 H), 7.82 (d, $J = 2.44$, 4 H), 7.71 (s, 2 H), 4.3–4.1 (m, 20 H), 2.94 (s, 4 H), 2–1.8 (m, 24 H), 1.62–1.38 (m, 40 H), 1.14–0.89 (m, 30 H); δ_C 156.2, 149.4, 149.2, 148.6, 131.4, 124.4, 124.1, 123.6, 122.5, 107.9, 107.7, 107.2, 106.8, 103.4, 69.8, 69.5, 69.4, 67.9, 31.1, 30.5, 29.1, 28.3, 22.5, 14.0. $C_{90}H_{130}O_{10}$ (1370.97): calcd. C 78.79, H 9.55; found C 79.02, H 9.52.

CONCLUSIONS

We have described morphology to control the molecular orientational and long range positional order of the triphenylene twins, particularly the emergence of polymorphism including the nematic phase. Indeed, we have prepared a variety of symmetrical and non-symmetrical twins with different peripheral alkoxy or branched tails. The two triphenylene moieties are tethered via rigid ethynyl-bridge spacer, the lower homologues show the nematic phase, and higher homologues show nematic and/or columnar mesophases. On the other hand, lower homologous of twin 4 having butadiynyl-bridge spacer shows nematic phase and higher homologous are crystalline solid. We found that the important factor on the mesomorphism of TP twins is the relative lengths between the rigid spacer and the β-substituted chain. Namely, β-substituted chain must be shorter than the spacer length. The effect of branched aliphatic chains on the mesomorphism was also discussed. The introduction of branched chains only into β-substituted positions does not prevent molecules from showing mesogenic phases, if the above rule on the relative lengths of β-substituted chain and the spacer is satisfied. These π-conjugated twins are model molecules, for oligomers and polymers for the molecular electronics (few nanometers) to supramolecular electronics (hundreds of nanometers).

ACKNOWLEDGMENT

SKV is very grateful to Prof. K. A. Suresh for his sustaining support for the research work and thankful to Dr. S. Krishna Prasad for helpful discussion. A fellowship by Japan Society for Promoting Science (JSPS), Japan is gratefully acknowledged.

REFERENCES

[1] Hoeben, F. J. M., Jonkheijm, P., Meijer, E. W., & Schenning, A. P. H. J. (2005). *Chem. Rev.*, *105*, 1491.
[2] Naoki, O. (2003). *DIC Technical Review*, *9*, 53; *Flat Panel Displays, Advanced Organic Materials*. (2000). Kelly, S. M. (Eds.), Royal Society of Chemistry.
[3] Chandrasekhar, S., Sadashiva, B. K., & Suresh, K. A. (1977). *Pramana*, *9*, 471.
[4] Warman, J. M., & Van de Craats, A. M. (2003). *Mol. Cryst. Liq. Cryst.*, *396*, 41.
[5] Van de Craats, A. M., & Warman, J. M. (2001). *Adv. Mater.*, *13*, 130.
[6] Van de Craats, A. M., Warman, J. M., Fechtenkoetter, A., Brand, J. D., Harbison, M. A., & Müllen, K. (1999). *Adv. Mater.*, *11*, 36.
[7] Struijk, C. W., Sieval, A. B., Dakhorst, J. E., Van Dijk, M., Kimkes, P., Koehorst, R. B., Donker, H., Schaafsma, T. J., Picken, S. J., Van de Craats, A. M., Warman, M., Zuilhof, H., & Sudholter, E. J. R. (2000). *J. Am. Chem. Soc.*, *122*, 11057.
[8] Monobe, H., Terasawa, N., Kiyohara, K., Shimizu, Y., Azehara, H., Nakasa, A., & Fujihira, M. (2004). *Mol. Cryst. Liq. Cryst.*, *412*, 1839.
[9] Zimmermann, S., Wendroff, J. H., & Weder, C. (2002). *Chem. Mater.*, *14*, 2218.
[10] Van de Craats, A. M., Stutzmann, N., Bunk, O., Nielsen, M. M., Watson, M., Müllen, K., Chanzy, H. D., Sirringhaus, H., & Friend, R. H. (2003). *Adv. Mater.*, *15*, 495.
[11] McCulloch, I., Weimin, Z., Heeney, M., Bailey, C., Giles, M., Graham, D., Shkunov, M., Sparrowe, D., & Tierney, T. (2003). *J. Mater. Chem.*, *13*, 2436.
[12] Schmidt-Mende, L., Fechtenkotter, A., Müllen, K., Moons, E., Friend, R. H., & MacKenzie, J. D. (2001). *Science*, *293*, 1119.
[13] Schouten, P. G., Warman, J. M., deHaas, M. P., Fox, M. A., & Pan, H. L. (1991). *Nature*, *353*, 736.
[14] Freudenmann, R., Behnisch, B., & Hanack, M. (2001). *J. Mater. Chem.*, *11*, 1618; Adam, D., Schuhmacher, P., Simmerer, J., Häussling, L., Siemensmeyer, K., Etzbach, K. H., Ringsdorf, H., & Haarer, D. (1994). *Nature*, *371*, 141.
[15] Seguy, I., Destruel, P., & Bock, H. (2000). *Synth. Met.*, *111*, 15.
[16] Kawata, K. (2002). *Chem Rec.*, *2*, 59.
[17] Okazaki, M., Kawata, K., Nishikawa, H., & Negoro, M. (2000). *Polym. Adv. Technol.*, *11*, 398.
[18] Mori, H., Itoh, Y., Nishiura, Y., Nakamura, T., & Shinagawa, Y. (1997). *Jpn. J. Apply. Phys.*, *36*, 143.
[19] Leenhouts, F. (2000). *Jpn. J. Apply. Phys.*, *39*, L471.
[20] Bushby, R. J., & Lozman, O. R. (2002). *Curr. Opin, Colloid Interface Sci.*, *7*, 343.
[21] Cammidge, A. N., & Bushby, R. J. (1998). In: *Hand Book of Liquid Crystals*, Vol. 2B, Demus, D., Goodby, J., Gray, G. W., Spiess, H. W., & Vill, V. (Eds.), Wiley-VCH: Weinheim, 693.
[22] Kumar, S. (2005). *Liq. Cryst.*, *32*, 1089.
[23] Laschat, S., Baro, A., Steinke, N., Giesselmann, F., Hagele, C., Scalia, G., Judele, R., Kapatsina, E., Sauer, S., Schreivogel, A., & Tosoni, M. (2007). *Angew. Chem. Int. Ed.*, *46*, 4832.

[24] Imrie, C. T., Lu, Z., Picken, S. J., & Yildirin, Z. (2007). *Chem. Comm.*, 1245, and reference cited therein.
[25] Boden, N., Bushby, R. J., Cammidge, A. N., & Martin, P. J. (1995). *J. Mater. Chem.*, *5*, 1857.
[26] Imrie, C. T., & Henderson, P. A. (2002). *Curr. Opin. Colloid Interface Sci.*, *7*, 298.
[27] Boden, N., Bushby, R. J., Cammidge, A. N., El-Mansoury, A., Martin, P., & Lu, Z. (1999). *J. Mater. Chem.*, *9*, 1391.
[28] Closs, F., Haubling, L., Henderson, P., Ringsdrof, H., & Schuhmacher, P. (1995). *J. Chem. Soc. Perkin Trans-1*, 829.
[29] Imrie, C. T., Karasz, E. F., & Attard, G. S. (1993). *Macromolecules*, *26*, 3803.
[30] Imrie, C. T., & Luckhurst, G. R. (1998). In: *Hand Book of Liquid Crystals*, Vol. 2B, Demus, D., Goodby, J., Gray, G. W., Spiess, H. W., & Vill, V. (Eds.), Wiley-VCH: Weinheim, 801.
[31] Lillya, C. P., & Murthy, Y. L. N. (1985). *Mol. Cryst. Liq. Cryst.*, *2*, 121.
[32] Whitesides, G. M., & Boncheva, M. (2002). *PNAS*, *99*(8), 4769.
[33] Kumar, S., & Varshney, S. K. (2002). *Org. Letts.*, *4*, 157.
[34] Kumar, S., & Varshney, S. K. (2001). *Liq. Cryst.*, *28*, 161.
[35] Novak, Z., Nemes, P., & Kotschy, A. (2004). *Org. Letts.*, *6*, 4917.
[36] Boden, N., Bushby, R. J., & Lu, Z. B. (1999). *Liq. Cryst.*, *26*(4), 495.
[37] Rego, J. A., Kumar, S., & Ringsdorf, H. (1996). *Chem. Mater.*, *8*, 1402.
[38] Guillaume, L., & Feldman, Ken S. (2002). In: *Modern Arene Chemistry*, Didier, Atruc (Eds.), Wiley-VCH: Weinhein, 479.
[39] Varshney, S. K., Yelammagad, C. V., & Takezoe, H. (2007). *Liq. Cryst.*, *34*(7), 787.
[40] Luu, T., Elliott, E., Slepkov, A. D., Eisler, S., McDonald, R., Hegmann, F. A., & Tykwinski, R. R. (2005). *Org. Letts.*, *7*(1), 51.
[41] Varshney, S. K., Shankar Rao, D. S., & Kumar, S. (2001). *Mol. Cryst. Liq. Cryst.*, *357*, 55.
[42] Chang, J. Y., Yeon, J. R., Shin, Y. S., Han, M. J., & Hong, S. (2000). *Chem. Mater.*, *12*, 1076.
[43] Urgaonkan, S., & Verkade, J. G. (2004). *J. Org. Chem.*, *69*, 5752.
[44] The distance two ends of terminal carbon atoms were measured from MM2 optimized models. Molecular modeling was performed using Chem3D Ultra 9.0 (Cambridge software) and ACD 3D v.4.0 (ACD Inc.)
[45] Ford, W. T., Sumner, L., Zhu, W., Chang, Y. H., Um, P., Choi, K. H., Heiney, P. A., & Maliszewsky, N. C. (1994). *New. J. Chem.*, *18*, 495.
[46] Varshney, S. K., Takezoe, H., & Rao, D. S. S. (2008). *Bull. Chem. Soc. Jpn.*, *80*(1), 163.
[47] Hassheider, T., Benning, S. A., Kitzerow, H., Achard, M., & Block, H. (2001). *Angew. Chem. Int. Ed.*, *40*, 2060.
[48] Sergeyev, S., Debever, O., Pouzet, E., & Geerts, Y. H. (2007). *J. Mater. Chem.*, *17*, 3002.